

How fast does water flow in carbon nanotubes?

Sridhar Kumar Kannam,^{1,a)} B. D. Todd,^{1,b)} J. S. Hansen,^{2,c)} and Peter J. Daivis^{3,d)}

¹Mathematics Discipline, Faculty of Engineering and Industrial Science, and Centre for Molecular Simulation, Swinburne University of Technology, Melbourne, Victoria 3122, Australia

²DNRF Center 'Glass and Time', IMFUFA, Department of Science, Systems and Models, Roskilde University, DK-4000 Roskilde, Denmark

³School of Applied Sciences, RMIT University, Melbourne, Victoria 3001, Australia

(Received 24 October 2012; accepted 9 February 2013; published online 1 March 2013)

The purpose of this paper is threefold. First, we review the existing literature on flow rates of water in carbon nanotubes. Data for the slip length which characterizes the flow rate are scattered over 5 orders of magnitude for nanotubes of diameter 0.81–10 nm. Second, we precisely compute the slip length using equilibrium molecular dynamics (EMD) simulations, from which the interfacial friction between water and carbon nanotubes can be found, and also via external field driven non-equilibrium molecular dynamics simulations (NEMD). We discuss some of the issues in simulation studies which may be reasons for the large disagreements reported. By using the EMD method friction coefficient to determine the slip length, we overcome the limitations of NEMD simulations. In NEMD simulations, for each tube we apply a range of external fields to check the linear response of the fluid to the field and reliably extrapolate the results for the slip length to values of the field corresponding to experimentally accessible pressure gradients. Finally, we comment on several issues concerning water flow rates in carbon nanotubes which may lead to some future research directions in this area.

© 2013 American Institute of Physics. [<http://dx.doi.org/10.1063/1.4793396>]

I. INTRODUCTION

The transport properties of water in nanopores are of both fundamental and practical interest. Water flow in carbon nanotubes (CNTs) has received significant attention over the last decade due to the importance of water and the unique properties of CNTs. Even though water is the most studied material on earth, its anomalous bulk properties are still surprising and properties of highly confined water are fascinating. On the other hand, CNTs possess unique properties such as having nanoscale diameters, ultra-smooth hydrophobic surfaces, and high aspect ratio. Hence, water flow in CNTs is a subject of intense research (see Refs. 1–9 and the references therein).

The flow rates of water in CNTs depend strongly on the slip length. Numerous experimental and simulation studies have been carried out in order to find the transport properties of water through CNTs.^{10–29,31–49} The flow enhancement results differ by 1–5 orders of magnitude compared to the classical no-slip flow predictions (see Fig. 1 and Table I). The slip length L_s and flow enhancement E for Hagen-Poiseuille flow are defined as follows:¹⁸

$$u_s = u(R) = L_s \left| \left(\frac{\partial u(r)}{\partial r} \right)_{r=R} \right|, \quad (1)$$

$$E = \frac{Q_{\text{slip}}}{Q_{\text{no-slip}}} = \left(1 + \frac{8L_s}{D} \right), \quad (2)$$

where u_s is the slip velocity (fluid velocity at the wall), Q_{slip} is the observed flow rate, $Q_{\text{no-slip}}$ is the expected flow rate using the no-slip boundary condition, and D is the diameter of the tube. For a given fluid-solid combination the slip length is a useful property, which is commonly quoted in the nanofluidics literature. Above a certain channel width/tube diameter the slip length is independent of the channel size. Using Eq. (2) one can estimate the flow enhancement given the slip length.

In 2005, Majumder *et al.*¹³ reported a slip length of 39–68 μm for a 7 nm diameter CNT in their experimental studies, which results in a flow enhancement of $(44\text{--}77) \times 10^3$. The following year, Holt *et al.*¹⁶ studied even smaller nanotube membranes and found 0.14–1.4 μm slip length for diameters 1.3–2.0 nm. These two studies, along with a simulation study by Hummer *et al.*¹⁰ in 2001, showing that water can be transported through a 0.81 nm diameter hydrophobic CNT, generated immense interest in the research community and hence numerous experimental and simulation studies have been undertaken, many with a special focus on the slip length. Majority of the subsequent studies have found smaller slip lengths and some have found just around ~ 10 nm slip length for the same diameter range tubes. In experimental studies, Whitby *et al.*¹⁸ found 113–177 nm slip length for a 44 nm diameter nanopipe. Sinha *et al.*³¹ found no significant deviation from classical behaviour for 200–300 nm diameter tubes. As the diameter of the tube increases, the curvature effects on the fluid transport diminish. Using a 10 nm diameter CNT membrane Du *et al.*¹⁷ found 485 μm slip length. Qin *et al.*¹⁹ found just 53–8 nm non-monotonic slip length for 0.81–1.59 nm diameter tubes (for diameters 0.81, 0.87, 0.89, 1.10, 1.42, 1.52, 1.59 nm the corresponding slip lengths are 53, 44.6, 29.3,

^{a)}Electronic mail: urssrisri@gmail.com.

^{b)}Electronic mail: btodd@swin.edu.au.

^{c)}Electronic mail: jschmidt@ruc.dk.

^{d)}Electronic mail: peter.daivis@rmit.edu.au.

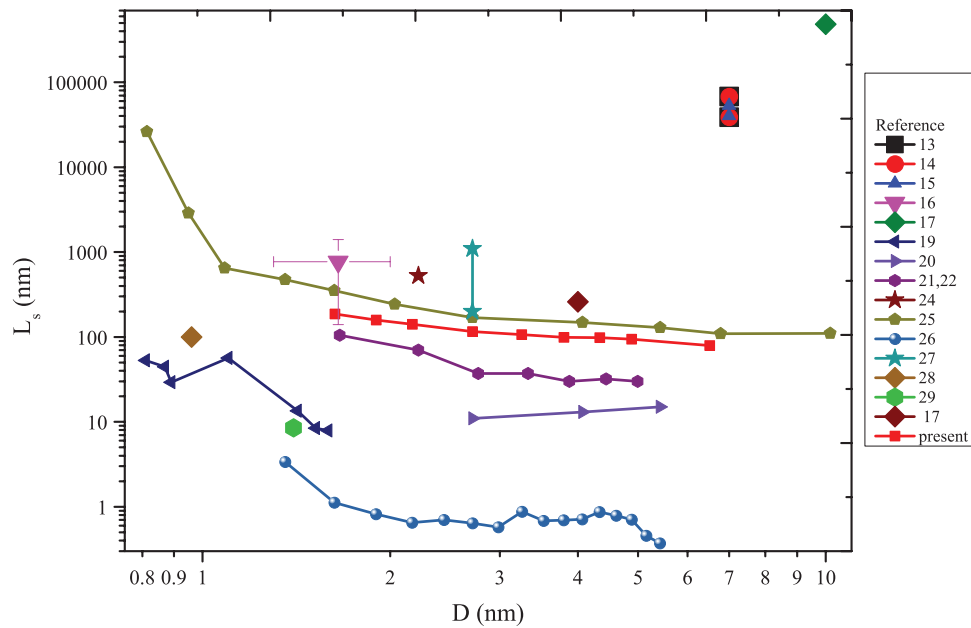


FIG. 1. Literature on the slip length of water in CNTs of diameter 0.81–10 nm. Our predictions are in red square symbols with a connected line. Notice the logarithmic scale on the y axis.

TABLE I. Literature on the slip length of water in CNTs and on a planar graphene surface. E, S, and T stand for experiment, simulation, and theory, respectively. The reader is suggested to refer to the original papers for details.

| No. | Reference | Year | Diameter (nm) | Slip length (nm) |
|-----|--|----------|------------------|---|
| 1 | Kotsalis <i>et al.</i> ²⁰ | 2004 (S) | 2.71, 4.07, 5.42 | 11, 13, 15 |
| 2 | Majumder <i>et al.</i> ¹³ | 2005 (E) | 7 | $(39-68) \times 10^3$ |
| 3 | Holt <i>et al.</i> ¹⁶ | 2006 (E) | 1.3–2.0 | 140–1400 |
| 4 | Thomas <i>et al.</i> ²² | 2008 (S) | 1.66–4.99 | 110–30 |
| 5 | Joseph <i>et al.</i> ²⁴ | 2008 (S) | 2.22 | 556 |
| 6 | Whitby <i>et al.</i> ¹⁸ | 2008 (E) | 44 | $(113 \pm 9)-(177 \pm 15)$ |
| 7 | Sinha <i>et al.</i> ³¹ | 2009 (E) | 200–300 | Negligible |
| 8 | Falk <i>et al.</i> ²⁵ | 2010 (S) | 1–10 | 500–120 |
| 9 | Thomas <i>et al.</i> ²¹ | 2010 (S) | 1.66–4.99 | 110–30 |
| 10 | Qin <i>et al.</i> ¹⁹ | 2011 (E) | 0.81–1.59 | 53–8 |
| 11 | Myers ²⁹ | 2011 (T) | 1.4, 40 | 8.5, 35 |
| 12 | Du <i>et al.</i> ¹⁷ | 2011 (S) | 4 | 260 |
| 13 | Du <i>et al.</i> ¹⁷ | 2011 (E) | 10 | 485×10^3 |
| 14 | Babu <i>et al.</i> ²⁶ | 2011 (S) | 0.81–5.42 | 6.5–1 |
| 15 | Majumder <i>et al.</i> ¹⁴ | 2011 (E) | 7 | $((40 \pm 18)-(53 \pm 14)) \times 10^3$ |
| 16 | Majumder <i>et al.</i> ¹⁵ | 2011 (E) | 7 | $(39-68) \times 10^3$ |
| 17 | Ma <i>et al.</i> ²⁷ | 2011 (S) | 2.71 | 200–1100 |
| 18 | Nicholls <i>et al.</i> ²⁸ | 2012 (S) | 0.96 | 100 |
| 19 | Present work | 2012 (S) | 1.62–6.5 | 180–75 |
| 1 | Koumoutsakos <i>et al.</i> ³⁴ | 2003 (S) | ∞ | 64 |
| 1 | Kotsalis ³³ | 2006 (S) | ∞ | 67 ± 45 |
| 2 | Thomas <i>et al.</i> ²² | 2008 (S) | ∞ | 30 |
| 3 | Maali <i>et al.</i> ³⁶ | 2008 (E) | ∞ | 8 ± 2 |
| 4 | Falk <i>et al.</i> ²⁵ | 2011 (S) | ∞ | 80 |
| 5 | Qin <i>et al.</i> ¹⁹ | 2011 (E) | ∞ | 10 |
| 6 | Babu <i>et al.</i> ²⁶ | 2011 (S) | ∞ | 1 |
| 7 | Xiong <i>et al.</i> ³⁸ | 2011 (S) | ∞ | 54 |
| 8 | Gu <i>et al.</i> ³⁷ | 2011 (S) | ∞ | 77 |
| 9 | Myers ²⁹ | 2011 (T) | ∞ | 35 |
| 10 | Kannam <i>et al.</i> ⁴⁹ | 2012 (S) | ∞ | 60 ± 6 |

56.6, 13.5, 8.4, 7.9 nm, respectively). In 2011, in their extended studies, Majumder *et al.*^{14,15} confirmed their earlier results from 2005. Thus far in experimental studies slip lengths varying over 5 orders of magnitude for tubes of diameters 0.81–10 nm have been reported.

During this time many molecular dynamics (MD) simulation studies have also been carried out due the feasibility of conducting simulations compared to the difficulty of performing nanoscale fluidic experiments. Walther *et al.*²⁰ found just 11, 13, 15 nm slip lengths for 2.71, 4.07, 5.42 nm diameter tubes, respectively. For 1.66–4.99 nm diameter tubes, Thomas *et al.*²² found monotonically decreasing slip length from 105 to 30 nm. This slip length approached 30 nm for larger diameter tubes and on a planar graphene surface. Later they found non-continuum (fluid structure dependent) and non-monotonic transport in the diameter range 0.83–1.66 nm with a slip length below 1000 nm.²³ They attribute the non-monotonic behaviour to the changing fluid structure. In an attempt to understand the mechanism of fast transport, Joseph *et al.*²⁴ found a slip length of 556 nm in a 2.17 nm diameter tube. Du *et al.*¹⁷ found 260 nm slip length for a 4 nm diameter tube. Recently, Falk *et al.*²⁵ and Babu *et al.*²⁶ found monotonically decreasing slip length as the tube diameter increases, but with a different magnitude. Falk *et al.*²⁵ found 2.6 μm to 120 nm slip length for tubes of diameter 0.81–7 nm, whereas Babu *et al.*²⁶ found just 3–0.3 nm for 0.83–5.42 nm diameter tubes. For a 2.72 nm diameter tube, Ma *et al.*²⁷ found 200–1100 nm slip length depending on the contact angle by varying the water-carbon interaction strength. While studying the effects of defects on the nanotube, Nicholls *et al.*²⁸ found a slip length of 100 nm for a 0.96 nm diameter defect free nanotube. Theoretically, using a reduced viscosity in the depletion layer near the nanotube surface, Myers²⁹ found a monotonically decreasing flow enhancement (not the slip length) as the tube diameter increases. For a 40 nm diameter tube they predicted a 35 nm slip length. The maximum limit to the enhancement predicted by the model is 50 for a 1.4 nm diameter tube with a slip length of 8.57 nm. In a recent simulation study with tube diameter range 1.09–1.62 nm, Wang *et al.*³⁰ found just 10–15 flow enhancement which is equivalent to a slip length of just a few nm. Some simulation studies have immersed the CNT in a water bath or connected the CNT to two water reservoirs and then applied a pressure gradient. For a given tube diameter, these studies have found CNT length affecting flow enhancement and attribute this to the entrance and exit effects at the ends of the CNT.^{28,46,47} In summary, simulation studies show slip lengths between ~ 1 and 1100 nm for the tube diameter range 0.81–7 nm.

Understanding the slip behaviour of water on a planar graphene surface is also an important problem. As mentioned before, as the diameter of the tube increases, the curvature effects diminish and the fluid confined in it behaves as it would confined in a planar graphene slit pore.^{22,25,50,51} Therefore, the slip length of water on a planar graphene surface serves as one extreme value of the slip length for CNTs. It is found that the minimum slip length we can expect for any diameter carbon nanotube is equal to or larger than the slip length of water on a graphene surface,^{22,25,50} although a few studies have found increasing friction (slip is inversely proportional

to the friction) as the tube diameter decreases.^{20,32,35} They have attributed this to the increasing confinement leading to a high surface to volume ratio. In Table I, we have also included the slip length of water on a planar graphene surface. As can be seen the data span the range ~ 1 –80 nm.

In this work, we address some of the issues present in the simulation studies which may be a reason for the disagreement in simulation results. We use EMD simulations to predict the interfacial friction between water and CNTs of various diameters. This friction coefficient is then used to determine the slip length. By taking this approach, we overcome the limitations of NEMD simulations. In NEMD simulations, for each tube we apply a range of external fields to determine the linear response of the fluid to the field and reliably extrapolate the results (slip length) to experimentally accessible pressure gradients.

II. METHODS AND RESULTS

We use flexible models for both water and CNTs. For water, we use the SPC/Fw model⁵² which has been shown to reproduce the transport properties such as diffusion and shear viscosity of liquid water close to experimental values.⁵³ CNTs are modelled using the Tersoff-Brenner second generation reactive empirical bond order potential (REBO).⁵⁴ The interactions between the oxygen atoms of the water molecules and carbon atoms of the CNTs are modelled using the Lennard-Jones potential with the parameters of Werder *et al.*⁴⁵ All Lennard-Jones interactions are truncated at a distance of 1 nm. Electrostatic interactions are handled using the Wolf method.^{55,56} The temperature is maintained at 300 K by applying the Nosé-Hoover thermostat to the CNT atoms, so that the heat produced by the viscous dissipation is conducted away through the wall. The overall water density in the tube is kept at 1000 kg/m³. At each state point, up to 20 independent simulations are carried out for up to 20 ns depending on the tube size and external field, using the leap-frog integration algorithm with a time step of ~ 1 fs. We have simulated nine single walled water filled CNTs of diameter 1.62–6.5 nm with vacuum outside. The length of the tubes vary from 7.37 nm to 2.45 nm from smaller to larger diameter and periodic boundary conditions are applied along the tube axial direction.

A. Slip length from interfacial friction coefficient: Equilibrium simulations

To find the flow rates and slip length using MD, it is a common practice to perform non-equilibrium simulations and analyze the velocity profiles. However, this method has a number of limitations intrinsic to it which we will comment on later (see also Ref. 49). One can alternatively determine the slip length from the Navier interfacial friction coefficient ξ_0 .⁵⁷

$$L_s = \frac{\eta_0}{\xi_0}, \quad (3)$$

where η_0 is the shear viscosity. Recently, we have provided a method for calculating the fluid-solid interfacial friction at a planar surface⁵⁸ and cylindrical geometry.⁵⁰ Here, we use

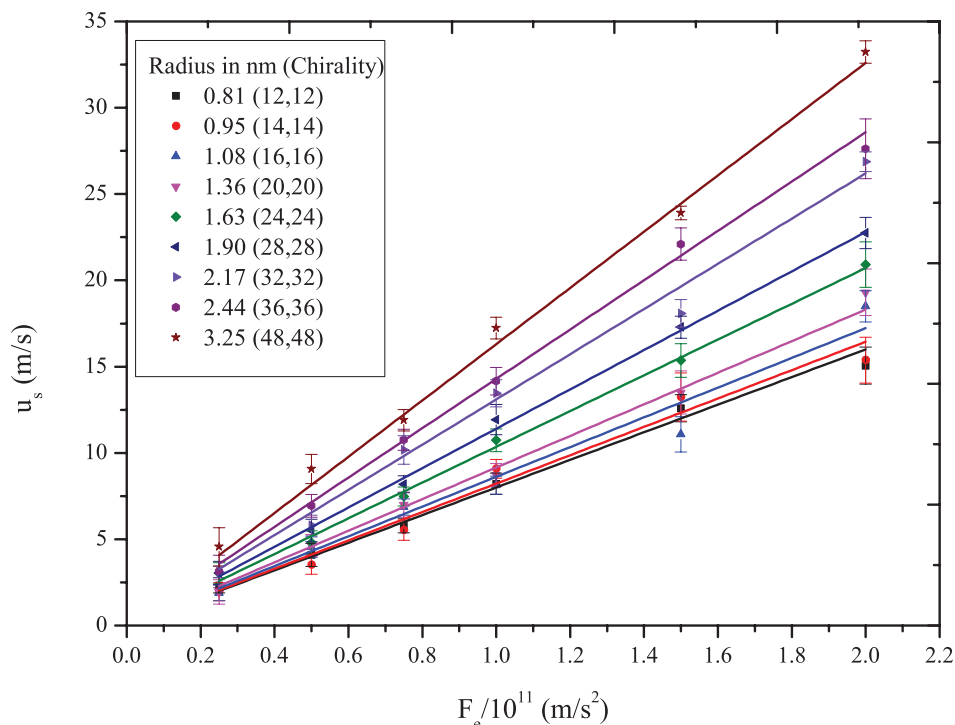


FIG. 2. The slip velocity against the external field in the low field range for different diameter CNTs. The continuous lines are linear fits to the data, with zero intercept on the y -axis.

this method to find the friction coefficient between water and CNTs of various diameters using equilibrium simulations. In brief, for each tube we choose a cylindrical fluid slab (annulus) of average width Δ of one molecular diameter adjacent to the CNT surface, i.e., $\Delta = 0.316$ nm (the van der Waals size of the water molecule in the SPC/Fw model⁵²). After equilibration, we evaluate the centre of mass (CM) velocity of the slab $u_{\text{slab}}(t)$ and wall-slab shearing force $F_z(t)$ in the axial direction, here the z direction. Using these two quantities, we evaluate the slab CM velocity autocorrelation function $C_{uu}(t) = \langle u_{\text{slab}}(0)u_{\text{slab}}(t) \rangle$ and the slab velocity-force cross correlation function $C_{uF_z}(t) = \langle u_{\text{slab}}(0)F_z(t) \rangle$, both of which are non-zero. The friction coefficient is then found via the relation $\tilde{C}_{uF_z}(s) = -\tilde{\zeta}(s)\tilde{C}_{uu}(s)$ in Laplace space. The details of the steps involved can be found in Ref. 58. We then find the slip length for each CNT by dividing the shear viscosity of bulk water by the corresponding friction coefficient of the tube^{25,50} (see Sec. III on shear viscosity).

B. Slip length from streaming velocity profiles: Non-equilibrium simulations

In non-equilibrium Poiseuille flow simulations, we drive the fluid by applying a range of constant external fields to all the atoms of water molecules. We fit the streaming velocities to a quadratic equation $u_z(r) = ar^2 + b$ by constraining the fit such that the parameters satisfy the shear viscosity of bulk water. Due to the high slip and small velocity difference from the centre to the solid surface, constraining the fit is necessary.^{22,49} Using the fitting parameters the slip length is found from its definition in Eq. (1). Note that a quadratic

velocity profile is generally valid for channels of width above roughly 5 molecular diameters.^{22,60,61}

In Fig. 2, we plot the slip velocity for each tube from the NEMD data as a function of external field at the low fields we have used. For each tube, we fit the data to a straight line with zero y -axis intercept (slip velocity). Even though these fields are equivalent to pressure gradients 2–3 orders of magnitude higher than those experimentally accessible, the linear increase in the fluid slip velocity with external field suggests that the results can be reliably extrapolated down to fields corresponding to experimentally accessible pressure drops which are generally below 1 atm.^{13,16,18} Note that in our simulations flow is generated by an external field and not by a pressure gradient in the axial direction.⁶⁰ As the difference in fluid velocity from the centre to the wall is very small, this slip velocity can be approximated to the fluid average velocity in the tube.

In Fig. 3, we plot the slip length for each tube from NEMD data as a function of external field. At low fields, where the fluid mean velocity is much smaller than the fluid thermal velocity, the slip length shows large uncertainties as expected. As we increase the field, the uncertainties in the fluid streaming velocity data decrease, as do the uncertainties in the slip length. In the low field range, the slip length is constant for each tube within statistical uncertainty. At a given low field, smaller diameter tubes show high slip length compared to the wider diameter tubes and the linear regime (where the slip length is constant) extends over a larger range of external field for smaller diameter tubes compared to the wider diameter tubes. With increasing field, wider diameter tubes begin to show the nonlinear behaviour for

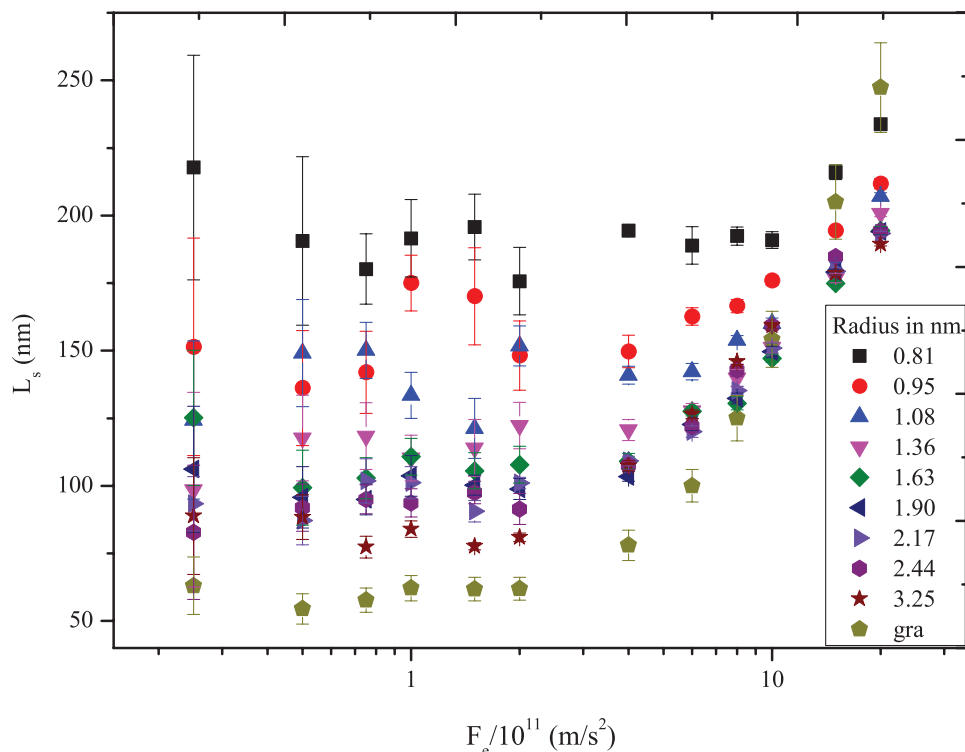


FIG. 3. The slip length against external field for different diameter CNTs. The plot also includes the slip length of water on a planar graphene surface (gra).⁴⁹

relatively small fields compared to the smaller diameter tubes. In Fig. 3, we also have included the slip length of water on a planar graphene surface.⁴⁹ As can be clearly seen, with increasing tube diameter, the water slip behaviour approaches what it would if confined in a planar graphene slit pore (tube

of infinite diameter). Thus, with increasing tube diameter, both the confinement and curvature effects become negligible, as one expects.

In Fig. 4 we plot the same slip length data as a function of tube diameter at different external fields. The plot also

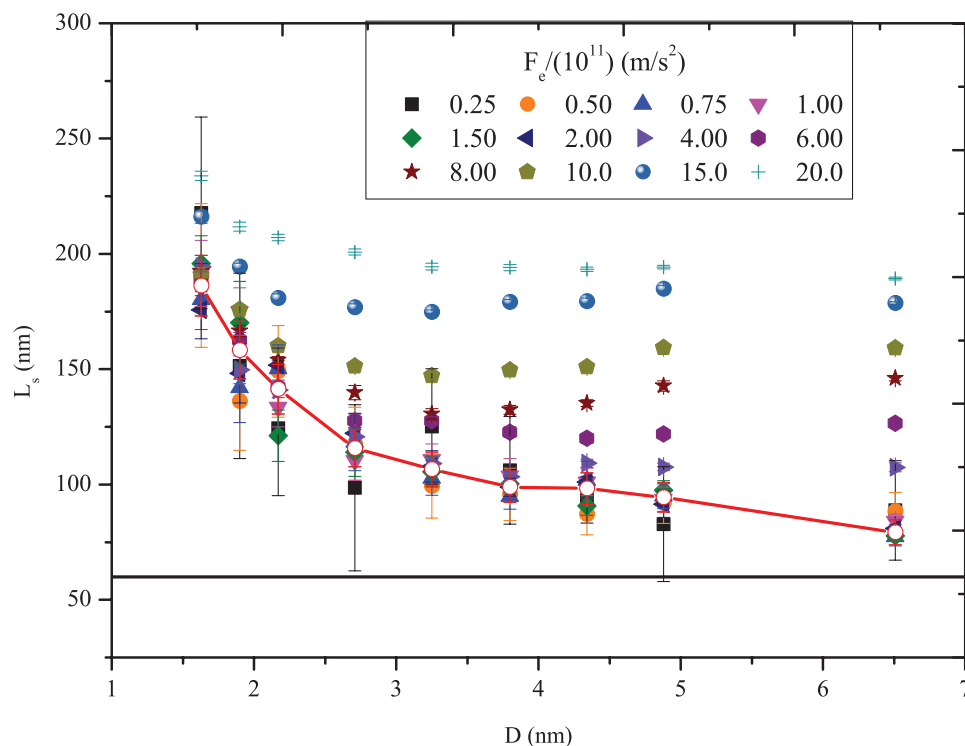


FIG. 4. The slip length against the diameter of CNTs at different external fields. The open red circles with a connected line are slip lengths measured using the fitting procedure described in the text. The black line at $60 (\pm 6)$ is the slip length of water on a planar graphene surface.⁴⁹

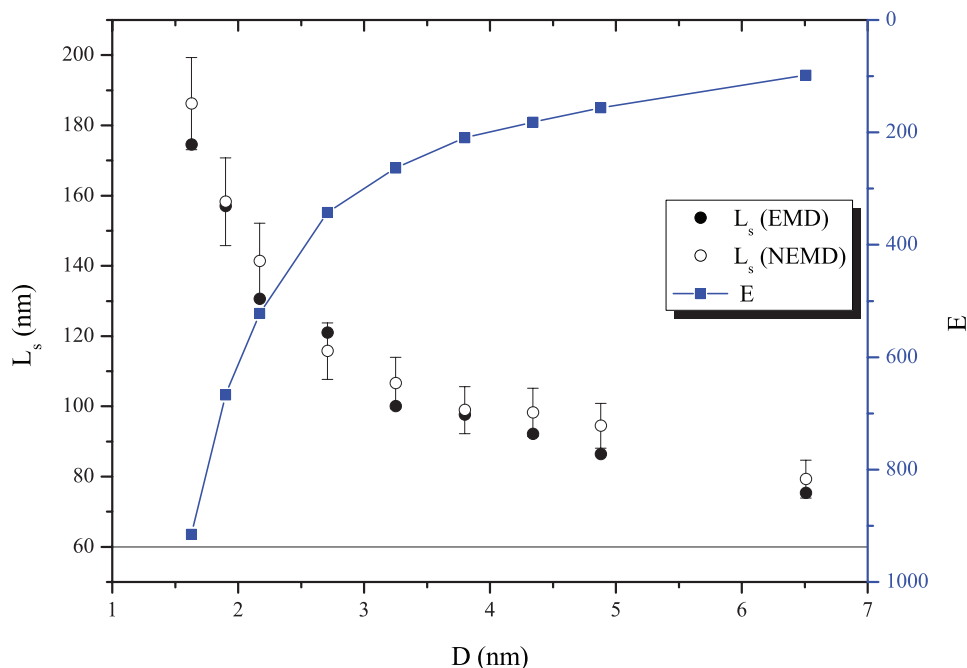


FIG. 5. The slip length predicted using the EMD and NEMD methods and flow enhancement (E) against the diameter of CNTs. The black line at $60 (\pm 6)$ is the slip length of water on a planar graphene surface.⁴⁹ The flow enhancement is calculated using the slip length from our EMD method.

includes open red circles with a connected line, which we explain in the following paragraph.

Using the slip modified Poiseuille flow Navier-Stokes solution (see Eq. (5) below) one can derive the following expression for slip length and interfacial friction between water and CNT⁴⁹

$$L_s = \frac{4m\eta_0}{\rho D} \quad \text{and} \quad \xi_0 = \frac{4m}{\rho D}, \quad (4)$$

where ρ is the fluid density and m is the slope obtained by plotting the slip velocity against the external field, in the low field range (linear regime). As extrapolating the slip length to linear regime fields from data in Fig. 3 becomes unreliable, we have used the following method to determine the slip length for each tube. For a given tube, we combine the slip velocity data at different external fields to get a reliable slip length. The slope m is determined from the linear fits to the slip velocity data in Fig. 2. The open red circles with a connected line in Fig. 4 represent the slip length determined by this method, and as can be seen it overlaps with the slip length data at low external fields within the statistical errors.⁴⁹

Slip lengths and flow rate enhancements predicted from EMD and NEMD are plotted as a function of CNT diameter in Fig. 5. Good agreement between both of the methods can be seen in the plot. The NEMD method required an order of magnitude higher computational time, as the simulations needed to be done at different external fields to check the linearity and to predict the slip length reliably by combining the data at different external fields.

The slip length is high in smaller diameter tubes and as the tube diameter increases, the slip length decreases monotonically and asymptotically approaches a constant value, which is equal to the slip length on a planar graphene

surface.⁴⁹ This trend is in qualitative agreement with the findings in Refs. 22, 25, and 50. Equivalently, the flow enhancement is very high in narrow diameter tubes and as the tube diameter increases, the flow enhancement decreases monotonically and the flow rates approach the Navier-Stokes prediction with the no-slip boundary condition for micrometer diameter tubes. For wider tubes of diameter in the micrometer range, the effect of slip on flow enhancement is negligible. Notice, the slip length still remains around 60 nm, but its effect on enhancement becomes negligible, see Eq. (2).

For a long time slip has been a controversial subject. Tubes in the micrometer diameter range were used in earlier experiments.⁵⁹ For such relatively wide tubes the effect of nanometer scale slip length on flow rates is negligible, and hence the results have supported the no-slip boundary condition, even if slip is present. These effects only become significant in nanometer diameter range pores.

We now compare our predictions with experimental results, see Fig. 1 and Table I. For tubes of diameter 1.63–2.17 nm, our predicted slip length is in the range of 180–145 nm, which is in agreement with the lower end of results by Holt *et al.*,¹⁶ who predict 140–1400 nm slip length for tubes of diameter 1.3–2.0 nm. For similar diameter tubes, the results of Qin *et al.*¹⁹ are just below 10 nm. We are unable to study tubes of larger diameter than those used here due to computational limitations. Our results suggest only around 60 nm slip length for tubes of diameter 7 nm and 10 nm and above, for which Majumder *et al.*^{13–15} measure slip lengths 4 orders of magnitude higher (3.9–6.8 μm) and Du *et al.*¹⁷ measured similar (485 μm) slip lengths. For a 44 nm diameter carbon nanopee Whitby *et al.*¹⁸ measured 113–117 nm slip length. For tubes of diameter 200–300 nm, our results suggest a flow enhancement of 2.6–3.4, which is close to a factor of 2 found by Sinha *et al.*³¹

Comparing our predictions with other simulation results, the variation of slip length with CNT diameter is in qualitative agreement with the predictions by Falk *et al.*²⁵ and Thomas *et al.*²² but quantitatively differ by a factor of 2. For tubes of diameter 1–7 nm Falk *et al.* predicted 500–120 nm slip length, and Thomas *et al.* predicted 125–30 nm slip length for tubes of diameter 1.66–4.99 nm, whereas we predict 180–75 nm slip length for tubes of diameter 1.66–6.5 nm. Other simulation results are scattered with around an order of magnitude deviation from our predictions. Again we refer to Fig. 1 and Table I. Some variation in simulation results is accounted for by the differences in the molecular models used to simulate the system and the simulation details.

III. DISCUSSION

We now briefly comment on several important issues in relation to the computation of flow rates of water in CNTs (and in general fluid flow rates in nanopores). We hope this will point to future research directions in this area.

The two key concepts in predicting nanofluidic flow rates are (i) the fluid effective shear viscosity and (ii) the fluid-solid slip length (boundary condition). Both of these concepts are usually defined using the uniform fluid density hypothesis, which breaks down at the nanoscale. From the macroscale down to around 4 nm channel width (around 10 fluid molecular diameters), the fluid shear viscosity and the predicted quadratic velocity profiles across the channel do not show any significant variation.^{60,61} Below this level of confinement the breakdown of the constant density assumption becomes significant. At what scale the classical hypothesis of constant density and constant viscosity breaks down is a general question and the transition is very weak and depends on the nature of both the fluid and solid.

For the effective shear viscosity of water, different studies have found increasing, decreasing, and non-monotonic variation with respect to the CNT diameter.^{19,22,26,39–42,44} Some publications report less than a factor of 2 variation^{19,22} and others report variation of 1–2 orders of magnitude.^{26,44} At this high level of confinement, the fluid becomes highly inhomogeneous, showing density oscillations across the whole channel,³⁰ which is likely to result in position dependent transport properties and non-local response functions. Hence, the transport coefficients such as shear viscosity become position dependent across the channel and for a complete description a non-local viscosity kernel in space is needed.^{62,63} The discrepancy in the shear viscosity of water confined in CNTs could be due to the breakdown of existing methods of defining and measuring viscosity for such tightly confined fluids, which are in general devised for bulk fluids.

The slip length of water has been reported even for 0.81 nm diameter tubes, which can accommodate only a single water molecule across the tube diameter. In such a 1D pore, water forms a single file molecular chain, and the fluid velocity profile is no longer well defined.^{60,61} The relation between the slip length and flow enhancement (Eq. (2)) is valid only when the classical Navier-Stokes quadratic velocity profile shifts upwards by the slip velocity (see Eq. (5)). Equation (2) and the definition of slip length itself breaks down when the inho-

mogeneity is strong. In this case, it is more useful to discuss transport through the pore in terms of permeability rather than slip flow.

MD simulations use empirical potentials to model the system and hence the reliability of any simulation results largely depends on the potential model and the parameters. Even though the water molecule is relatively simple, the collective properties are very complex and hence several models have been proposed for water (e.g., Guillot⁶⁴ listed 46 models), each one predicting certain properties correctly under certain conditions only. Most of these models are parameterized using the bulk water experimental properties of interest. Therefore, the validity of these models at the nanoscale is questionable, which may be another reason for the large gap between experimental and simulation flow rates.

The interaction strength between water and wall carbon atoms is also very important. Hummer *et al.*,¹⁰ found that even a small change in the water oxygen-carbon interaction strength results in drying-to-wetting transitions of water in CNTs of diameter 0.83 nm. Recently, Melillo *et al.*⁴⁸ also found that a 0.075 kcal/mol change in the interaction strength can affect the flux by a large amount. Werder *et al.*⁴⁵ studied the contact angle of water on a graphite surface with varying interaction strength. Most of the subsequent simulation studies use the parameters from their study, which produce the experimental contact angle of water on a graphite surface. How well these parameters can capture the interaction between water and CNTs of varying diameter is yet to be studied.

Modelling the electrostatic interactions is also an important issue. The Ewald summation method was developed for systems that are periodic in 3 directions⁶⁵ and later it was extended for systems that are periodic in 2 directions (e.g., fluids confined in slit pores).⁶⁶ In systems such as water confined in CNTs, the system is periodic only in 1 direction. For very narrow tubes, the applicability of the Ewald technique to handle electrostatics has yet to be examined in detail. Other methods such as the Wolf^{22,55} and smooth cutoff^{20,33,45,70} are also often used for water confined in CNTs. In the literature, some spurious effects resulting from mishandling of the electrostatic interactions for water-CNT systems have also been shown.^{67–69}

Thermostating the system is another important issue.⁷¹ When a fluid is confined in a pore within a solid pore, the natural way to maintain the desired temperature for the fluid is to thermostat the solid at that temperature and keep the fluid unthermostated, so that the viscous heat generated in the fluid is conducted away through the fluid-solid interface. In this way the intrinsic dynamics of fluid atoms are unaffected. Thermostating the fluid directly to maintain the desired temperature can affect the results depending on the property of interest (e.g., as mentioned before, the slip length is very sensitive to the fluid velocity gradient (strain rate) at the wall).^{22,49} For graphene and CNTs, the Tersoff-Brenner potential is widely used when predicting their structural, elastic, and mechanical properties. This is a non-additive pair potential and takes the nature of chemical bonding and environment into account in a complex way. In nanofluidic simulation studies, allowing flexibility of the tube by using the REBO potential increases the computational time by an order of magnitude.⁷² To avoid this,

and for simplicity, most simulation studies keep the carbon atoms of the nanotube fixed and thermostat the water directly to maintain the desired temperature. As mentioned above, this may have an undesired artificial effect on the streaming velocity profiles.⁷¹ Sokhan *et al.*⁷² found a 20% increase in the flux/flow rates for methane with flexible CNTs compared to rigid nanotubes. Care must be taken in applying the thermostat depending on the sensitivity of the property of interest. Proposing a simplified potential (and parameters) for CNTs by comparing against the REBO potential, where the properties of interest are of fluids, would overcome this problem.

Some limitations of NEMD simulations also contribute to the discrepancy in simulation results. The thermal velocity of water at room temperature is approximately 340 m/s. As NEMD simulations can generally be done only for a few nanoseconds with a time step of around a femtosecond, the pressure gradients or external fields used are 4–5 orders of magnitude higher than the experimental values in order to have the fluid mean velocity comparable to the thermal velocity, i.e., to have a reasonable signal to noise ratio.⁵⁹ The typical mean fluid velocities in experiments are smaller than 0.01 m/s. At such high fields, the linearity of Eq. (1) may not hold and the flux/slip length determined may not correspond to the value found under experimental conditions. As shown previously the slip length remains constant⁵⁰ (flux increases linearly with pressure gradient)^{30,43} in the low field/shear rate range, above which it increases rapidly with the field.⁵¹ As one does not have any prior knowledge about the extent of the linear regime, a few test simulations should be done to check for a linear response to the field. The field should be low enough to ensure a linear response and high enough to get a reasonable velocity signal. Moreover, an external field, which gives the limiting slip for a tube, may not give the limiting slip length for a different diameter tube for the same fluid and solid.⁵⁰ For very large slippage, NEMD simulations cannot resolve the small difference in velocity between the centre of the channel and the wall.⁴⁹ As shown before, the slip length is very sensitive to the fluid strain rate at the wall, and using NEMD one cannot predict the slip length reliably when the slip length is high.

To elaborate on this point, we note that water flow in carbon nanotubes is often described as a plug flow, meaning a flat velocity (Euler flow) profile across the tube. On the other hand, the slip modified Poiseuille flow solution is

$$u_z(r) = \left(\frac{\rho F_e}{4\eta_0} \right) (R^2 - r^2) + u_s. \quad (5)$$

Therefore, the only difference compared to the no-slip solution is the slip velocity added to the no-slip boundary solution, i.e., the effect of slip is only an upward shift in the velocity profile. The velocity difference from centre to the wall (proportional to the external field) still remains the same and hence so too does the curvature of the flow profile. Compared to the fields used to drive the fluid confined between Lennard-Jones walls (which are normally attractive and highly corrugated resulting in a small or zero slip),⁵⁹ for water in nanotubes we use 1–2 orders of magnitude smaller fields as the slip is high which results in high mean velocities. This small field decreases the velocity difference of the fluid from the

centre to the wall proportionately. As mentioned above, one cannot resolve the velocity difference below approximately a few m/s using NEMD. These two reasons make the velocity profiles apparently look flat cross the channel (plug like). Therefore, describing the velocity profile as plug-like can be misleading sometimes for very high slip systems as water in CNTs.

The effect of a change in the shear viscosity on flow enhancement is not clear. A decrease in effective shear viscosity due to the confinement may or may not increase the average flow rate. A decrease in effective shear viscosity increases the fluid velocity gradient at the wall, to which the slip length is inversely proportional. So, a decrease in effective shear viscosity does not necessarily mean increase in flow enhancement when the pressure gradient is kept constant.

The uncertainty in defining the actual tube diameter (available volume) becomes comparable to the tube diameter itself for very narrow tubes. The one atomic diameter uncertainty (0.34 nm van der Waals size of the carbon atoms) in the tube diameter makes a significant difference in the measured flow enhancement for small diameter tubes. For example, if the distance between the centre of mass of the opposite carbon atoms (D) on a CNT is 0.81 nm, defining the tube diameter as 0.81 nm has a 0.34 nm uncertainty, which is 42%. Different variants in defining the tube diameter are D , $D-0.34$, $D-(0.34 + \sigma_O)/2$, where σ_O is the van der Waals diameter of the oxygen atom in a given water model and sometimes the wall positions are taken from where the density of fluid has a finite value.

The issue of entrance and exit effects which resulted in a tube length dependent flow enhancement also has to be examined in detail.^{28,30,46,47}

Finally, as defined sometimes, the slip length is not the additional length at which the no-slip boundary condition holds, neither is it the length from the wall at which the extrapolated velocity profile reaches zero. The slip length is the additional length from the wall at which the tangent to the fluid velocity at the wall is extrapolated to reach zero relative tangential velocity between fluid and solid. As the slip length is very sensitive, specifying the boundary condition and quantifying the flow enhancement using the slip length should be done carefully.

IV. CONCLUSION

To conclude, we have predicted the slip length of water in CNTs using equilibrium simulations to compute the interfacial friction of water in CNTs and extensive field driven nonequilibrium simulations. Due to the high sensitivity of the slip length to the streaming velocity profiles, computing the slip using the NEMD methods is unreliable if it is not done with sufficient care and it is computationally intensive. We find a monotonically decreasing 180–75 nm slip length for tubes of diameter 1.66–6.5 nm. The slip length is high in small diameter tubes where the curvature and confinement effects are large. As the diameter of the tube increases, the slip length decreases monotonically and it asymptotically approaches a constant value (60 ± 6 nm) around the slip length of water on a planar graphene surface. In other words, the flow

enhancement is very high in narrow tubes and as the diameter of the tube increases, the flow rate slowly approaches the classical Navier-Stokes prediction with the no slip boundary condition (and no significant enhancement). For tubes of diameter 1.66–6.5 nm our results suggest a flow enhancement of around 870–90. For a 1.0 μm diameter tube, the slip length of 60 nm results in only an enhancement of 1.5. The effects of both confinement and curvature on slip become negligible at around ~ 10 nm, and the slip length becomes independent of the tube diameter around and above ~ 10 nm, which is still in the nanoscale regime. We have briefly reviewed the literature on flow rates of water in CNTs highlighting the many pitfalls related to this problem, and suggested some future research directions that will lead to a better understanding of water transport in CNTs.

ACKNOWLEDGMENTS

This project was supported by the Victorian Partnership for Advanced Computing HPC Facility and Support Services and an award under the Merit Allocation Scheme on the NCI National Facility at the ANU. J. S. Hansen wishes to acknowledge Lundbeckfonden for supporting this work as a part of Grant No. R49-A5634.

- ¹H. Verweij, M. Schillo, and J. Li, *Small* **3**, 1996 (2007).
- ²M. Whitby and N. Quirke, *Nat. Nanotechnol.* **2**, 87 (2007).
- ³M. Whitby and N. Quirke, *Handbook of Nanophysics* (CRC, 2010), Chap. 11.
- ⁴H. Fang, R. Wan, X. Gong, H. Lu, and S. Li, *J. Phys.: D. Appl. Phys.* **41**, 103002 (2008).
- ⁵J. K. Holt, *Microfluid. Nanofluid.* **5**, 425 (2008).
- ⁶J. K. Holt, *Adv. Mater.* **21**, 3542 (2009).
- ⁷A. Noy, H. G. Park, F. Fornasiero, J. K. Holt, C. P. Grigoropoulos, and O. Bakajina, *Nano Today* **2**, 22 (2007).
- ⁸A. Alexiadis and S. Kassinos, *Chem. Rev.* **108**, 5014 (2008).
- ⁹J. W. Choi, M. Alexandrova, and H. G. Park, *Carbon Nanotubes Applications on Electron Devices* (InTech, 2011), Chap. 18.
- ¹⁰G. Hummer, J. C. Rasaiah, and J. P. Noworyta, *Nature (London)* **414**, 188 (2001).
- ¹¹A. Kalra, S. Garde, and G. Hummer, *Proc. Natl. Acad. Sci. U.S.A.* **100**, 10175 (2003).
- ¹²B. Corry, *J. Phys. Chem. B* **112**, 1427 (2008).
- ¹³M. Majumder, N. Chopra, R. Andrews, and B. J. Hinds, *Nature (London)* **438**, 44 (2005).
- ¹⁴M. Majumder, N. Chopra, and B. J. Hinds, *ACS Nano* **5**, 3867 (2011).
- ¹⁵M. Majumder and B. Corry, *Chem. Commun.* **47**, 7683 (2011).
- ¹⁶J. K. Holt, H. G. Park, Y. Wang, M. Stadermann, A. B. Artyukhin, C. P. Grigoropoulos, A. Noy, and O. Bakajin, *Science* **312**, 1034 (2006).
- ¹⁷F. Du, L. Qu, Z. Xia, L. Feng, and L. Dai, *Langmuir* **27**, 8437 (2011).
- ¹⁸M. Whitby, L. Cagnon, M. Thanou, and N. Quirke, *Nano Lett.* **8**, 2632 (2008).
- ¹⁹X. Qin, Q. Yuan, Y. Zhao, S. Xie, and Z. Liu, *Nano Lett.* **11**, 2173 (2011).
- ²⁰E. M. Kotsalis, J. H. Walther, and P. Koumoutsakos, *Int. J. Multiphase Flow* **30**, 995 (2004).
- ²¹J. A. Thomas, A. J. H. McGaughey, and O. K. Arnebeck, *Int. J. Therm. Sci.* **49**, 281 (2010).
- ²²J. A. Thomas and A. J. H. McGaughey, *Nano Lett.* **8**, 2788 (2008).
- ²³J. A. Thomas and A. J. H. McGaughey, *Phys. Rev. Lett.* **102**, 184502 (2009).
- ²⁴S. Joseph and N. R. Aluru, *Nano Lett.* **8**, 452 (2008).
- ²⁵K. Falk, F. Sedlmeier, L. Joly, R. R. Netz, and L. Bocquet, *Nano Lett.* **10**, 4067 (2010).
- ²⁶J. S. Babu and S. P. Sathian, *J. Chem. Phys.* **134**, 194509 (2011).
- ²⁷M. D. Ma, L. Shen, J. Sheridan, J. Z. Liu, C. Chen, and Q. Zheng, *Phys. Rev. E* **83**, 036316 (2011).
- ²⁸W. D. Nicholls, M. K. Borg, D. A. Lockerby, and J. M. Reese, *Mol. Simul.* **38**, 781 (2012).
- ²⁹T. G. Myers, *Microfluid. Nanofluid.* **10**, 1141 (2011).
- ³⁰L. Wang, R. S. Dumont, and J. M. Dickson, *J. Chem. Phys.* **137**, 044102 (2012).
- ³¹S. Sinha, M. P. Rossi, D. Mattia, Y. Godotsi, and H. H. Bau, *Phys. Fluids* **19**, 013603 (2007).
- ³²S. C. Kassinos, J. H. Walther, E. Kotsalis, and P. Koumoutsakos, *Lect. Notes Comput. Sci. Eng.* **39**, 215 (2004).
- ³³E. M. Kotsalis, "Multiscale modeling and simulation of fullerenes in liquids," Ph.D. dissertation (ETH, Zurich, 2006).
- ³⁴P. Koumoutsakos, R. L. Jaffe, T. Werder, and J. H. Walther, *Nanotechnology* **1**, 148 (2003), <http://www.nsti.org/procs/Nanotech2003v1/8/T23.01>.
- ³⁵J. Hanasaki and A. Nakatani, *J. Chem. Phys.* **124**, 144708 (2006).
- ³⁶A. Maali, T. C. Bouhacina, and H. Kellay, *App. Phys. Lett.* **92**, 053101 (2008).
- ³⁷X. Gu and M. Chen, *App. Phys. Lett.* **99**, 063101 (2011).
- ³⁸W. Xiong, J. Z. Liu, M. Ma, Z. Xu, J. Sheridan, and Q. Zheng, *Phys. Rev. E* **84**, 056329 (2011).
- ³⁹H. Ye, H. Zhang, Z. Zhang, and Y. Zheng, *Nanoscale Res. Lett.* **6**, 87 (2011).
- ⁴⁰Y. Liu and Q. Wang, *Phys. Rev. B* **72**, 085420 (2005).
- ⁴¹Y. Liu, Q. Wang, T. Wu, and L. Zhang, *J. Chem. Phys.* **123**, 234701 (2005).
- ⁴²H. Zhang, H. Ye, Y. Zheng, and Z. Zhang, *Microfluid. Nanofluid.* **10**, 403 (2011).
- ⁴³F. Zhu, E. Tajkhorshid, and K. Schulten, *Biophys. J.* **83**, 154 (2002).
- ⁴⁴X. Chen, G. Cao, A. Han, V. K. Punyamurtula, L. Liu, P. J. Culligan, T. Kim, and Y. Qiao, *Nano Lett.* **8**, 2988 (2008).
- ⁴⁵T. Werder, J. H. Walther, R. L. Jaffe, T. Halicioglu, and P. Koumoutsakos, *J. Phys. Chem. B* **107**, 1345 (2003).
- ⁴⁶D. Mattiall and F. Calabro, *Microfluid. Nanofluid.* **13**, 125 (2012).
- ⁴⁷J. Su and H. Guo, *J. Phys. Chem. B* **116**, 5925 (2012).
- ⁴⁸M. Melillo, F. Zhu, M. A. Snyder, and J. Mittal, *J. Phys. Chem. Lett.* **2**, 2978 (2011).
- ⁴⁹S. K. Kannam, B. D. Todd, J. S. Hansen, and P. J. Daivis, *J. Chem. Phys.* **136**, 024705 (2012).
- ⁵⁰S. K. Kannam, B. D. Todd, J. S. Hansen, and P. J. Daivis, *J. Chem. Phys.* **136**, 244704 (2012).
- ⁵¹S. K. Kannam, B. D. Todd, J. S. Hansen, and P. J. Daivis, *J. Chem. Phys.* **135**, 144701 (2011).
- ⁵²Y. Wu, H. L. Tepper, and G. A. Voth, *J. Chem. Phys.* **124**, 024503 (2006).
- ⁵³G. Raabe and R. J. Sadus, *J. Chem. Phys.* **137**, 104512 (2012).
- ⁵⁴D. W. Brenner, O. A. Shenderova, J. A. Harrison, S. J. Stuart, B. Ni, and S. B. Sinnott, *J. Phys.: Condens. Matter* **14**, 783 (2002).
- ⁵⁵D. Wolf, P. Koblinski, S. R. Phillpot, and J. Eggebrecht, *J. Chem. Phys.* **110**, 8254 (1999).
- ⁵⁶C. J. Fennel and J. D. Gezelter, *J. Chem. Phys.* **124**, 234104 (2006).
- ⁵⁷C. L. M. H. Navier, *Mem. Acad. Sci. Inst. Fr.* **6**, 389 (1823).
- ⁵⁸J. S. Hansen, B. D. Todd, and P. J. Daivis, *Phys. Rev. E* **84**, 016313 (2011).
- ⁵⁹E. Lauga, M. P. Brenner, and H. A. Stone, *Experimental Fluid Dynamics* (Springer, New York, 2007).
- ⁶⁰K. P. Travis, B. D. Todd, and D. J. Evans, *Phys. Rev. E* **55**, 4288 (1997).
- ⁶¹K. P. Travis and K. E. Gubbins, *J. Chem. Phys.* **112**, 1984 (2000).
- ⁶²B. D. Todd and J. S. Hansen, *Phys. Rev. E* **78**, 051202 (2008).
- ⁶³B. D. Todd, J. S. Hansen, and P. J. Daivis, *Phys. Rev. Lett.* **100**, 195901 (2008).
- ⁶⁴B. Guillot, *J. Mol. Liq.* **101**, 219 (2002).
- ⁶⁵P. P. Ewald, *Ann. Phys.* **369**, 253 (1921).
- ⁶⁶I. C. Yeh and M. L. Berkowitz, *J. Chem. Phys.* **111**, 3155 (1999).
- ⁶⁷J. W. Ekkabut, M. S. Miettinen, C. Dias, and M. Karttunen, *Nat. Nanotechnol.* **5**, 555 (2010).
- ⁶⁸D. J. Bonthuis, K. Falk, C. N. Kaplan, D. Horinek, A. N. Berker, L. Bocquet, and R. R. Netz, *Phys. Rev. Lett.* **105**, 209401 (2010).
- ⁶⁹M. E. Suk and N. R. Aluru, *Phys. Rev. Lett.* **105**, 209402 (2010).
- ⁷⁰J. S. Hansen, T. B. Schroder, and J. C. Dyre, *J. Phys. Chem. B* **116**, 5738 (2012).
- ⁷¹S. Bernardi, B. D. Todd, and D. J. Searles, *J. Chem. Phys.* **132**, 244706 (2010).
- ⁷²V. P. Sokhan, D. Nicholson, and N. Quirke, *J. Chem. Phys.* **120**, 3855 (2004).